Picosecond Photolyses of Six-Coordinated Iron(II) Porphyrins: Formation and Decay of an Excited-State Five-Coordinated Species

Douglas Taube, Teddy G. Traylor,* Douglas Magde,* Kevin Walda, and Jikun Luo

Contribution from the Department of Chemistry, University of California, San Diego, 9500 Gilman Drive, La Jolla, California 92093-0506. *Received November 14, 1991. Revised Manuscript Received July 14, 1992*

Abstract: The picosecond photolysis of protoheme dimethyl ester bis(*tert*-butyl isocyanide) in pure *tert*-butyl isocyanide or in toluene results in loss of one isocyanide to produce an electronically excited five-coordinated species. The excited state decays to ground-state five-coordinated heme within 40 ps. In contrast to chelated protoheme–*tert*-butyl isocyanide or imidazole–protoheme dimethyl ester–*tert*-butyl isocyanide, no cage return is seen. The heme–*t*-BuNC returns to heme–(*t*-BuNC)$_2$ in a slower concentration dependent process having a bimolecular rate constant of 2.5×10^8 M^{-1} s^{-1}. Similar results were obtained with methyl isocyanide. With the larger isocyanides 5α-cholestan-3α-isocyanide and the 3β isomer the excited states return to the six-coordinated state with only a few percent of ground-state five-coordinated heme formation. This behavior is attributed to a faster decay of the excited state resulting from an interaction of the heme with the cholestane backbone. We conclude that excited-state five-coordinated hemes do not add ligands. The rate of excited-state decay depends upon the nature of the retained ligand (faster for Hm–imidazole than for Hm–isocyanide), but the spectra of the excited states seem to be very similar.

Introduction

The mechanisms of ligand binding to ferrous hemes and heme proteins have been investigated for many years.[1] Slow (ms to μs) photolysis studies corresponded well with stopped flow studies and established that, in complexes or hemeproteins having an imidazole (B) and a second ligand (L) such as CO, NO, O_2, or RNC, photolysis dissociates the second ligand.[2] The development

$$\mathrm{BHmL} \underset{k_{rec}}{\overset{h\nu}{\rightleftharpoons}} \mathrm{BHm} + \mathrm{L} \qquad (1)$$

of picosecond spectroscopy allowed such processes to be studied in more detail[3-12] and established that the photolysis occurs in less than 1 ps[10] to produce intermediate geminate states in which ligand rebinding competes with diffusion. In simple heme complexes (BHmL) there is one geminate state[11] (eq 2) and in hemeproteins (BHm'L) there are at least two (eq 3).[5,6,10,11]

$$\mathrm{BHmL} \underset{k_{-1}}{\overset{h\nu}{\rightleftharpoons}} [\mathrm{BHm\ L}] \underset{k_{-2}}{\overset{k_2}{\rightleftharpoons}} \mathrm{BHm} + \mathrm{L} \qquad (2)$$

$$\mathrm{BHm'L} \underset{k_{-1}}{\overset{h\nu}{\rightleftharpoons}} [\mathrm{BHm'\ L}] \underset{k_{-2}}{\overset{k_2}{\rightleftharpoons}} [\mathrm{BHm'} \| \mathrm{L}] \underset{k_{-3}}{\overset{k_3}{\rightleftharpoons}} \mathrm{BHm'} + \mathrm{L} \qquad (3)$$

On the picosecond time scale there are always excited-state decay processes, and these can interfere with attempts to follow geminate rebinding. The picosecond or subpicosecond photolyses of heme protein–ligand or model imidazole–heme–ligand complexes first produce UV–vis difference spectra which have broad absorbances in the 440–480-nm range,[10-12] usually thought to correspond to a mixture of excited-state and ground-state five-coordinated heme (BHm). The long wavelength part (450–480 nm) decays to $\Delta A = 0$ at 480 nm with a lifetime (τ) of 1–2 ps. Geminate processes of diffusion (k_2) and rebinding (k_{-1}) often have lifetimes of ~10 ps and thus it is usually assumed that, after ~4 ps, only geminate ground-state processes are occurring.[10]

$$\mathrm{BHmL} \underset{k^*_{-1}}{\overset{h\nu}{\rightleftharpoons}} [\mathrm{BHm^*\ L}] \xrightarrow{k^*} [\mathrm{BHm\ L}] \rightarrow \mathrm{BHm} + \mathrm{L} \qquad (4)$$

It is difficult to separate these processes completely and to determine whether the excited state decays to ground state (k^*) or returns to six-coordinated heme (k^*_{-1}). We have recently observed that photolysis of protoheme dimethyl ester bis(*tert*-butyl isocyanide) also produces the 440–480-nm band which decays in the picosecond time scale. However, in this case ground-state

$$\mathrm{Hm(CNR)_2} \xrightarrow{h\nu} [\mathrm{RNCHm^*\ CNR}] \xrightarrow{k^*} [\mathrm{RNCHm\ CNR}] \qquad (5)$$

five-coordinated heme absorbs around 402 nm.[13] This provides an ideal system to study the decay of excited-state five-coordinated heme to ground-state five-coordinated heme because the five-coordinated ground-state, excited-state, and six-coordinated hemes absorb at very different wavelengths (402, ~450, 432 nm). We

(1) Antonini, E.; Brunori, M. *Hemoglobin and Myoglobin and Their Reactions with Ligands*; North-Holland Publishing Co.: Amsterdam, 1971.
(2) Gibson, Q. H. *Prog. Biophys., Biophys. Chem.* **1959**, *9*, 1–53.
(3) Marden, M. C.; Hazard, III, E. S.; Gibson, Q. H. *Biochemistry* **1986**, *25*, 2786–2792.
(4) (a) Moore, J. N.; Hansen, P. A.; Hochstrasser, R. M. *Chem. Phys. Lett.* **1987**, *138*, 110–114. (b) Anfinrud, P. A.; Han, C.; Hochstrasser, R. M. *Proc. Natl. Acad. Sci. U.S.A.* **1989**, *86*, 8387–8391.
(5) Doster, W.; Bowne, S. F.; Frauenfelder, H.; Reinisch, L.; Shyamsunder, E. *J. Mol. Biol.* **1987**, *194*, 299–312.
(6) (a) Alberding, N.; Austin, R. H.; Chan, S. S.; Eisenstein, L.; Frauenfelder, H.; Good, D.; Kaufmann, K.; Marden, M. C.; Nordlund, T.; Reinisch, L.; Reynolds, A. H.; Sorensen, L. B.; Wagner, G. C.; Yue, K. T. *Biophys. J.* **1978**, *24*, 319–334. (b) Marden, M. C. *Eur. J. Biochem.* **1982**, *128*, 399–404. (c) Ansari, A.; DiIorio, E. E.; Dlott, D.D.; Frauenfelder, H.; Iben, I. E. T.; Langer, P.; Roder, H.; Sauke, T. B.; Shyamsunder, E. *Biochemistry* **1986**, *25*, 3139–3146.
(7) Duddell, D. A.; Morris, R. J.; Richards, J. T. *J. Chem. Soc., Chem. Commun.* **1979**, 75–76.
(8) Nöe, L. J.; Eisert, W. G.; Rentzepis, P. M. *Proc. Natl. Acad. Sci. U.S.A.* **1978**, *75*, 573–577.
(9) (a) Greene, B. I.; Hochstrasser, R. M.; Weisman, R. B.; Eaton, W. A. *Proc. Natl. Acad. Sci. U.S.A.* **1978**, *75*, 5255–5259. (b) Anfinrud, P. A.; Han, C.; Hochstrasser, R. M. *Proc. Natl. Acad. Sci. U.S.A.* **1989**, *86*, 8387–8391.
(10) (a) Petrich, J. W.; Poyart, C.; Martin, J. L. *Biochemistry* **1988**, *27*, 4049–4060. (b) Martin, J. L.; Migus, A.; Poyart, C.; Lecarpentier, Y.; Astier, R.; Antonette, A. *Proc. Natl. Acad. Sci. U.S.A.* **1983**, *80*, 173–177. (c) Martin, J. L.; Migus, A.; Poyart, C.; Lecarpentier, Y.; Astier, R.; Antonetti, A. *EMBO J.* **1983**, *2*, 1815–1819. (d) Petrich, J. W.; Martin, J. L. *Chem. Phys.* **1989**, *131*, 31–47.
(11) (a) Traylor, T. G.; Magde, D.; Taube, D. J.; Jongeward, K. A. *J. Am. Chem. Soc.* **1987**, *109*, 5864–5865. (b) Jongeward, K. A.; Magde, D.; Taube, D. J.; Marsters, J. C.; Sharma, V. S. *J. Am. Chem. Soc.* **1988**, *110*, 380–387. (c) Traylor, T. G.; Magde, D.; Taube, D. J.; Jongeward, K. A.; Bandyopadhyay, D.; Luo, J.; Walda, K. N. *J. Am. Chem. Soc.* **1992**, *114*, 417–429. (d) Traylor, T. G.; Taube, D. J.; Jongeward, K. A.; Magde, D. *J. Am. Chem. Soc.* **1990**, *112*, 6875–6880. (e) Mincey, T.; Traylor, T. G. *J. Am. Chem. Soc.* **1979**, *101*, 765–766.
(12) Rodriguez, J.; Kirmaier, C.; Holten, D. *J. Am. Chem. Soc.* **1989**, *111*, 6500–6506.

0002-7863/92/1514-9182$03.00/0

have taken advantage of these differences to study the photochemistry of $Hm(CNR)_2$ in detail and find a large difference between this system and ImHmCNR.

Experimental Section

Instrumentation. Time resolved spectra and single wavelength kinetic curves were obtained using picosecond and nanosecond laser systems previously described.[11a] Static UV–vis spectra were recorded on a Kontron Uvicon 810 instrument.

Materials. Methyl isocyanide was prepared by the literature procedure. Preparations of 5α-cholestan-3α-isocyanide (αChNC) and 5α-cholestan-3β isocyanide (βChNC) are described elsewhere.[13a] Both *tert*-butyl isocyanide (Fluka) and 1,1,3,3-tetramethylbutyl isocyanide (*t*-octyl NC) (Aldrich) were purchased. Methyl isocyanide (MeNC) and *tert*-butyl isocyanide (*t*-BuNC) were distilled often to assure purity. Protohemin dimethyl ester chloride and its reduced form [e.g., $Hm(RNC)_2$] were prepared according to literature preparations.[13] Toluene (Fisher) was distilled over $LiAlH_4$ under Ar. Light mineral oil (Whiteworth) was used without purification. Sodium dithionite was also purchased from Aldrich.

Ru(II) tetra(*p*-isopropylphenyl)porphyrin-CO was prepared by the recorded procedure[14,15] and chromatographed on silica gel with dichloromethane elution. Solutions in toluene, methanol, or hexanes were prepared by dissolving the complex in the solvent and subjecting it to 4 freeze–pump–thaw cycles then adding 0.01 M *t*-BuNC which converted the CO complex to the RuHm $(t\text{-BuNC})_2$, λ_{max} = 420 nm. Picosecond and nanosecond photolysis of this compound resulted in a first order decay with a rate constant of 1.1×10^6 s^{-1}. This rate was independent of *t*-BuNC concentration (10^{-3}–0.025 M) and showed a concomitant phosphorescence at 630–730 nm. No ligand photolysis was seen.

Samples Preparation. *Pure Isocyanide Solvents.* Protoheme dimethyl ester chloride ($PHDME^+Cl^-$) was dissolved in a minimum volume of dichloromethane and added to neat methyl or *tert*-butyl isocyanide (3 mL) until the absorbance of the Soret maximum was about 0.7 in a 2-mm cell. The solution was transferred to a tonometer containing a freshly made zinc amalgam. The sample was degassed by several freeze–pump–thaw cycles and then placed under argon. The sample was allowed to stir overnight to insure complete reduction to the ferrous heme and then cannulated into a degassed 2-mm quartz cuvette for kinetic analysis.

Toluene and Methylcyclohexane Solvents. Protoheme dimethyl ester chloride ($PHDME^+Cl^-$) was dissolved in a minimum volume of dichloromethane and added to toluene (2 mL) until the absorbance of the Soret maximum was about 2.1 in a 2-mm cell. The solution was degassed by passing argon through for 2 h. Alkyl isocyanide was added (2 μL of *t*-BuNC, 1 μL of MeNC, 5 mg of 5α-cholestan-3α-NC or 5α-cholestan-3β-NC). The concentrated heme solution was reduced by addition of saturated solution of sodium dithionite/18-crown-6/methanol (SDT, 1–2 μL)[11e] and stirring for 1 h. The reduced concentrated solution was diluted to proper concentration (6 mL, A_{Soret} = 1.6, [RNC] = $1–3 \times 10^{-3}$ M) with degassed toluene. The reduced protoheme dimethyl ester–$(RNC)_2$ was identified by the sharp Soret absorbance at 433 nm (ϵ = 250000 M^{-1} cm^{-1}). The sample was stored in a small test tube sealed by rubber septum under argon for kinetic analysis. Samples in methylcyclohexane were similarly prepared.

Mineral Oil Solvent. $PHDME^+Cl^-$ was reduced in 50/50 toluene/*t*-BuNC (v/v) using a Zn amalgam. This solution was anaerobically added to argon saturated mineral oil so the Soret absorbance at 433 nm was ~1.5. The resulting [*t*-BuNC] was 0.8 M.

Adamantane Heme-RNC in Toluene. Adamantane hemin chloride[13b] was dissolved in a minimum volume of dichloromethane and added to toluene (2 mL) until the absorbance of the Soret maximum was about 1.5 in 2-mm quartz cell (Precision). The solution was deoxygenated by bubbling Ar through it for 2 h. One equivalent of 5α-cholestan-3α-NC was added to it. The heme solution was reduced with freshly made saturated solution of sodium dithionite 18-crown-6/methanol, and the UV–vis spectrum of the five-coordinated adamantane heme-αChNC was recorded. With excess of 5α-cholestan-3α-NC (8×10^{-4} M), adamantane heme-bis(αChNC) was formed, and the UV–vis spectrum was recorded. Subtracting the spectrum of six-coordinated heme from the five-coordinated heme complex gives the static difference heme spectrum.

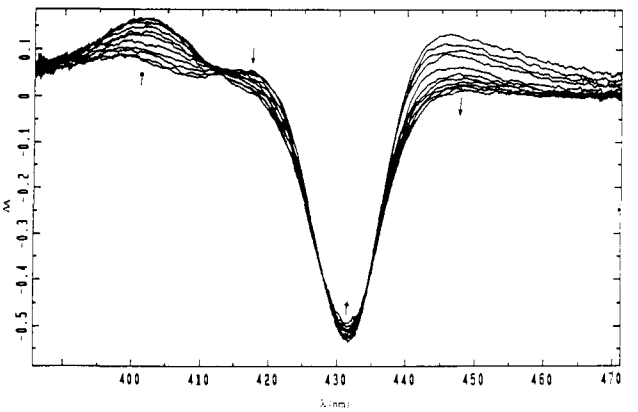

Figure 1. Picosecond transient absorption difference spectra for $PHDME(t\text{-BuNC})_2$ in neat *t*-BuNC after subpicosecond photolysis. [Hm] = 1×10^{-5} M, [*t*-BuNC] = 8.7 M. The change in absorbance is plotted versus wavelength as a function of time delay between the pump and probe pulse. The curves were obtained at 0, 2, 4, 6, 10, 14, 18, 22, 27, 32, 37, and 42 ps after photolysis. Photolysis energy was 60 μJ at 314 nm in this and subsequent figures.

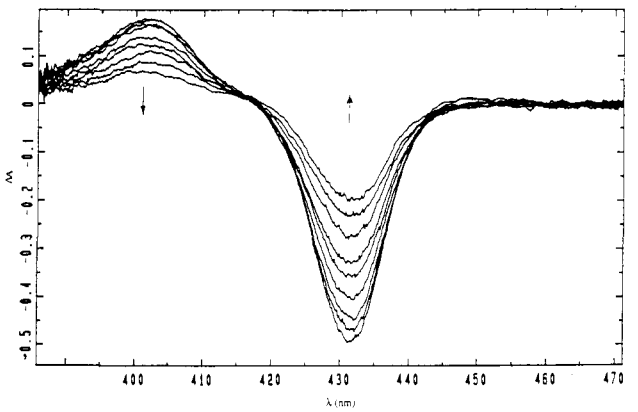

Figure 2. Picosecond transient absorption difference spectra for $PHDME(t\text{-BuNC})_2$ in neat *t*-BuNC after subpicosecond photolysis. A continuation of Figure 1. The curves were obtained at 42, 50, 75, 100, 125, 150, 200, 250, and 300 ps after photolysis.

Kinetic Methods. Bimolecular combination rates were determined by observing both the disappearance of the five-coordinated heme (405 nm) and the appearance of the six-coordinated heme after nanosecond photolysis (432 nm). The bimolecular rate constants were obtained from the slope of the plot of observed rate versus ligand concentration, over a range (1×10^{-3}–0.12 M) in which ligand concentration is in sufficient excess to assure pseudo-first-order kinetics. Picosecond data were obtained using instrumentation and sample flow techiques previously described.[11b]

Results

The spectrum of $PHDME(t\text{-BuNC})_2$ in toluene shows four peaks (relative absorbances in parentheses): 432 (1), 410 (0.23), 533 (0.09), and 562 (0.08). Figure 1 shows a series of difference spectra [(spectrum at *t*) − (spectrum before photolysis)] taken after picosecond photolysis of this complex in neat *tert*-butyl isocyanide. Zero time for the decay process is the point of largest excursion at 432 nm. This figure, taken only to 42 ps, shows initial loss of the 432-nm band, indicating the breaking of at least one Fe–CNR bond, with simultaneous appearance of a broad band 445–470 nm. During 42 ps the 450-nm band completely disappears with a first-order rate constant of 8×10^{10} s^{-1}, the same rate constant which characterizes the rise of a new peak at 402 nm.

Figure 2 is a continuation of Figure 1. The absorbance at 402 nm and that at 432 nm disappear, with the same rate constant, 4.3×10^9 s^{-1}, returning the sample to $Hm(CNR)_2$. Figure 3 shows a series of spectra taken as above, but the toluene solution con-

(13) (a) Jikun Luo, Ph.D. Thesis UCSD 1992. (b) Traylor, T. G.; Tsuchiya, S.; Campbell, D.; Mitchell, M. Stynes, D.; Koga, N. *J. Am. Chem. Soc.* **1985**, *107*, 604–614.

(14) Antipas, A.; Buchler, J. W.; Gouterman, M.; Smith, P. D. *J. Am. Chem. Soc.* **1978**, *100*, 3015–3024.

(15) Tait, C. D.; Holten, D.; Barley, M. H.; Dolphin, D. James, B. R. *J. Am. Chem. Soc.* **1985**, *107*, 1930–1934.

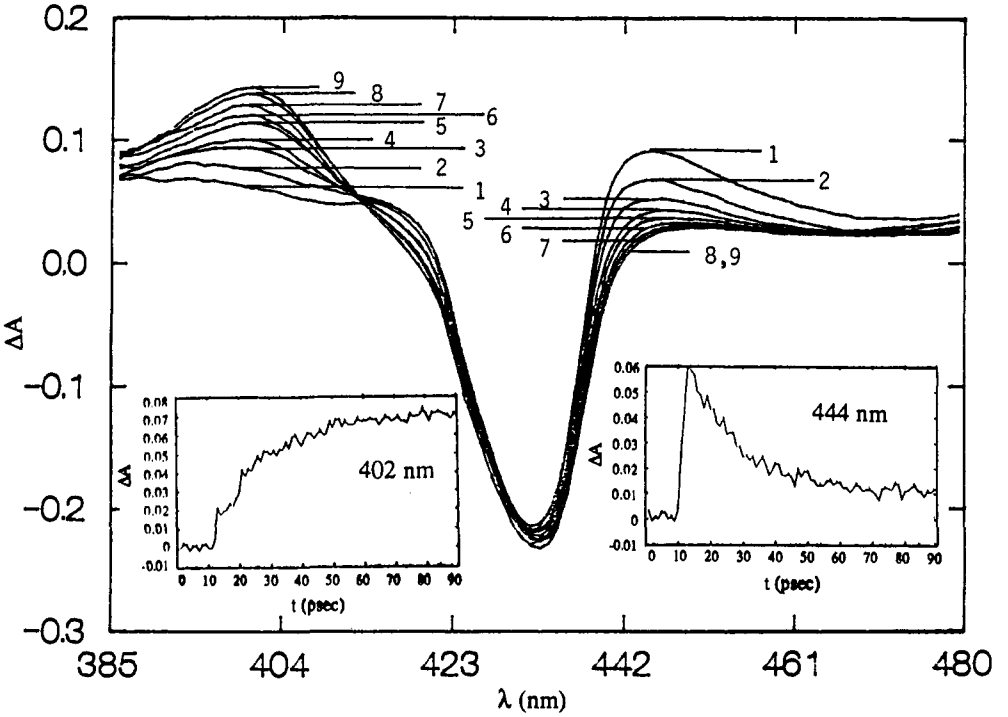

Figure 3. Picosecond transient absorption spectra for protoheme dimethyl ester (t-BuNC)$_2$ in toluene, [Heme] = 1×10^{-5} M, [t-BuNC] = 3×10^{-3} M. The absorbance change is plotted vs wavelength as a function of time delay between the pump and probe pulses. The numbers 1–9 label the curves recorded at 2, 6, 10, 14, 18, 22, 26, 32, and 38 ps after photolysis. The insets show the absorbance change vs time at 402 and 444 nm. The recombination rate of 5.5×10^{10} s^{-1} was observed at both wavelengths. No recovery of the six-coordinated heme at 432 nm was observed to 200 ps, the longest time in this experiment.

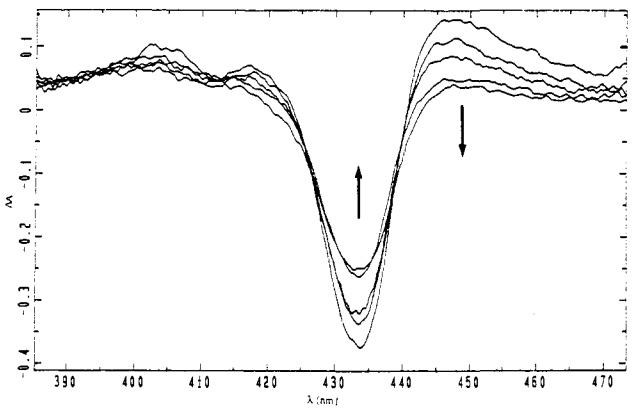

Figure 4. Picosecond transient absorption spectra of protoheme dimethyl ester bis(*tert*-butyl isocyanide) in mineral oil, [Heme] = 1×10^{-5} M, [t-BuNC] = 0.8 M. Times for the absorbance increase at 433 nm are 0, 2, 5, 10, and 20 ps.

tained 10^{-3} M t-BuNC. The rate constant for the fast reaction taken from the curves in Figure 3 is the same as that in Figure 1, but the return is absent on this time scale. Therefore the second process (Figure 2) is bimolecular.

In the more viscous solvent mineral oil there is evidence (Figure 4) of return of t-BuNC to the starting complex in competition with decay of the excited-state five-coordinated RNCHm* to ground-state RNCHm. This may be explained in terms of a retardation of k_2, the diffusion rate, by an increase in viscosity. Thus the RNCHm* decays in part before it leaves the contact pair. The ground-state contact pair is also expected to give more return in this viscous medium. Thus retarding k_2 by increasing viscosity or by increasing the size of the isocyanide increases the amount of geminate return by allowing more ground-state contact pair formation. It is also possible that both changes cause the rate of excited-state relaxation to increase through solvation complex formation and energy transfer.

No cage return after photolysis of Hm(MeNC)$_2$ in toluene was observed, and this was further demonstrated by picosecond photolysis of PHDME(MeNC)$_2$ in tetrahydrofuran solvent. The spectra between 0 and 40 ps are shown in Figure 5. This change is identical to that in toluene, and it has a similar rate. However, subsequent spectra (40–3000 ps) shown in Figure 6 shows the formation of absorbance with a maximum at 418 nm. We attribute this to formation of the THF–HmCNR complex and write these processes as shown below. The rate of the slower process is too small to be cage collapse to this species. Photolysis of

$$\text{Hm(MeNC)}_2 \xrightarrow{h\nu} [\text{HmMeNC*\ MeNC}] \xrightarrow{\sim 4\times 10^{10}} \text{HmCNMe+\ MeNC} \quad (6)$$

$$\text{HmCNMe} + \text{THF} \rightarrow \text{THF–HmCNMe} \quad (7)$$

heme-bis(αChNC) showed a small amount of the 402-nm absorption (Figure 7) and a predominate geminate recombination from 445 to 432 nm. Rate constants for changes of the 432- and 445-nm absorbances were the same, 8×10^{10} s^{-1}, and there was 95% return. Similar results (not shown) were obtained for the (βChNC) isomer. To test an intermediate size isocyanide, the PHDME (1,1,3,3-tetramethylbutyl isocyanide) was photolyzed. As Figure 8 illustrates, the spectral evolution is complicated, indicating predominant appearance of the 402-nm peak with simultaneous appearance of a small amount of return at 432 nm.

Bimolecular rate constants were determined at low ($\sim 10^{-3}$ M) concentrations of *tert*-butyl isocyanide. Figure 9 displays a plot of pseudo-first-order rate constants versus t-BuNC concentrations. Similar data were obtained for MeNC. The bimolecular rate constants, obtained from the slopes, are 2.5×10^8 and 2.8×10^8 M^{-1} s^{-1} for t-BuNC and MeNC, respectively.

To identify the 402-nm absorbance we recorded the static difference spectra of the mono and bis isocyanide complexes of adamantane heme (not shown).[13a] This heme is sterically hindered allowing the monoisocyanide complex to be formed.[13b] This was compared with the difference spectrum shown in Figure 10. After correction for differences of about 10 nm between protohemes

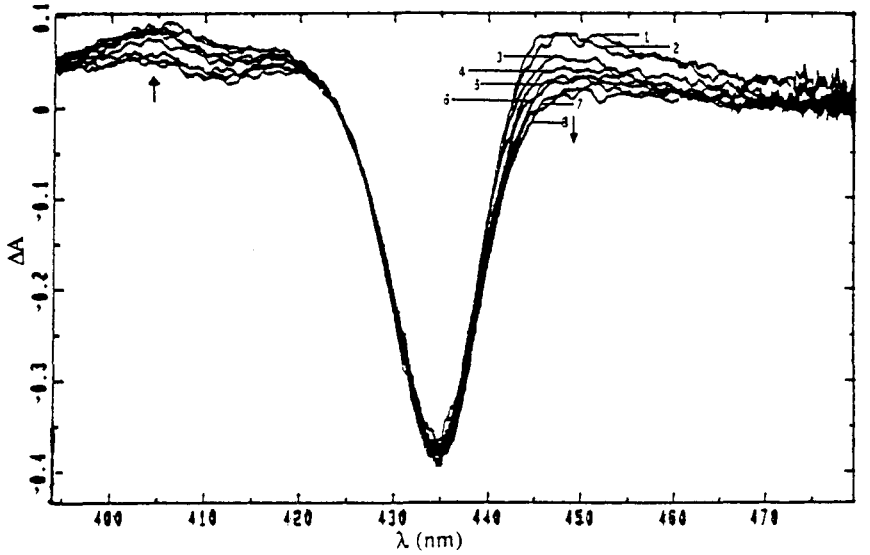

Figure 5. Picosecond transient absorption spectra for protoheme dimethyl ester bis(methyl isocyanide) in 90/10 THF/MeNC, [Heme] = 1×10^{-5} M, [MeNC] = 1.78 M. The numbers 1–8 label the curves recorded at 0, 2, 7, 10, 15, 20, 30, and 40 ps after photolysis. The rate constant for disappearance of absorbance at 450 nm and the appearance of absorbance at 405 nm was 5.2×10^{10} s^{-1}. No recovery of the six-coordinated PHDME$(MeNC)_2$ was observed.

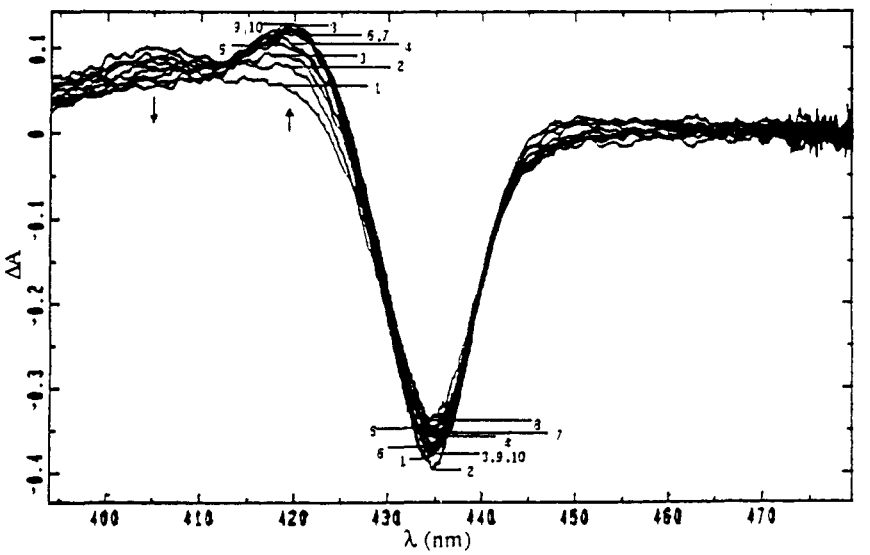

Figure 6. Picosecond transient absorption spectra for protoheme dimethyl ester bis(methyl isocyanide) in 90/10 THF/MeNC, [Heme] = 1×10^{-5} M, [MeNC] = 1.78 M. The numbers 1–10 label the curves recorded at 40, 50, 75, 100, 125, 150, 175, 200, 250, and 300 ps after photolysis. The rate of the disappearance of absorbance at 405 nm and the appearance of absorbance at 418 nm was 2×10^{10} s^{-1}. No recovery of the six-coordinated PHDME $(MeNC)_2$ was observed to 3000 ps, the longest time in this experiment.

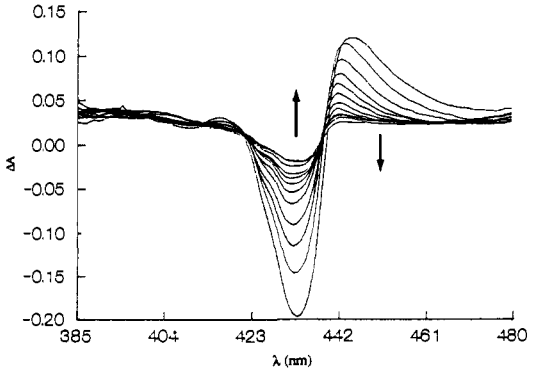

Figure 7. Picosecond transient absorption difference spectra for PHDME(5α-cholestan-3α-NC)$_2$ in toluene after subpicosecond photolysis. [Hm] = 1×10^{-5} M, [5α-cholestan-3α-NC] = 3×10^{-3} M. The times for the spectral changes are 0, 5, 8, 11, 14, 17, 23, 26, 29, 32, and 35 ps after photolysis.

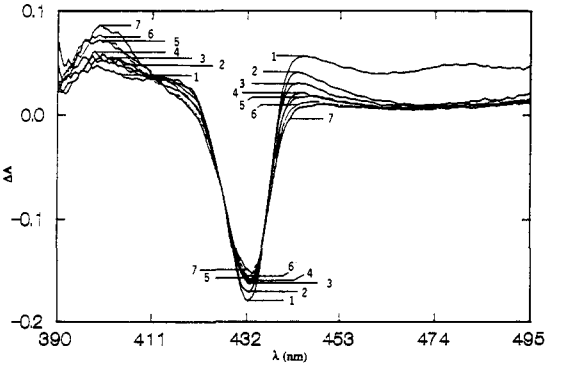

Figure 8. Picosecond transient absorption difference spectra for PHDME(1,1,3,3-tetramethylbutyl NC)$_2$ in toluene after subpicosecond photolysis. [Hm] = 1×10^{-5} M, [1,1,3,3-tetramethylbutyl NC] = 3×10^{-3} M. The numbers 1–7 label the curves obtained at 0, 6, 10, 13, 16, 19, and 22 ps after photolysis.

and mesohemes these two spectra correspond accurately, demonstrating that the 402-nm band corresponds to HmCNR.

Discussion

Although some six-coordinated metalloporphyrins such as Ru(II) tetraphenylporphyrin do not dissociate a ligand upon photolysis but simply decay to the ground states,[16] the iron porphyrins invariably dissociate one ligand as indicated in eq 1.[10,16,17] We are able to clearly separate the excited-state decay from ligand return because the five-coordinated heme–isocyanide complex absorbs at 402 nm and has no absorbance in the 450–470-nm range. The initial photoprocess involves ligand dissociation as indicated by the negative absorbance change at 432 nm, the Soret band for the $Hm(RNC)_2$. The ground-state five-coordinated

$$\begin{array}{ccccc} \text{RNC—Hm—CNR} & \xrightarrow{h\nu} & \text{[RNC—Hm* CNR]} & \xrightarrow{k_2} & \text{RNCHm* + CNR} \\ \uparrow & & \downarrow k^* & & \downarrow k^* \\ & \xleftarrow{k_{-1}} & \text{[RNCHm CNR]} & & \text{RNCHm} \end{array} \quad (8)$$

HmCNR complex is not formed directly since the 402-nm absorbance of this species is not formed initially. In the case of MeNC and *t*-BuNC the absorbance for HmCNR appears at the same rate as that for the disappearance of the long wavelength absorbance. This indicates initial formation of an excited-state five-coordinated species (HmCNR*) which decays with a rate constant of about 8×10^{10} s^{-1} to the ground-state five-coordinated species (HmCNR) without rebinding.

Nature of the Excited-State Species. The long wavelength absorbance of HmCN*t*-Bu* disappears with a half-life of 8.5 ps. In order to obtain the spectrum of HmCN*t*-Bu* we subtract the spectrum at zero time from that at about 5 half-lives (42 ps) and show this difference spectrum in Figure 10. We also show in Figure 11 the difference spectrum from the photolysis of 1,2-dimethylimidazole protoheme dimethyl ester-*t*-BuNC at zero time and 50 ps, the end of the long wavelength decay in that system. The corresponding difference spectrum between $t = 90$ picoseconds and $t = 0$ for the photolysis of myoglobin-CO is shown in Figure 12.

$$Hm(CNt\text{-}Bu)_2 \xrightarrow{h\nu} [t\text{-BuNCHm* } t\text{-BuNC}] \xrightarrow{k^*} t\text{-BuNCHm} + t\text{-BuNC} \quad (9)$$

$$MbCO \xrightarrow{h\nu} [Mb^* CO] \xrightarrow{k^*} Mb + CO \quad (10)$$

$$1,2\text{-DMImCN}t\text{-Bu} \xrightarrow{h\nu} [1,2\text{-DMImHm* CN}t\text{-Bu}] \rightarrow [1,2\text{-DMImHm CN}t\text{-Bu}] \quad (11)$$

All three spectra are characterized by a peak at ~450 nm. The two RNCHm spectra also have peaks at 420 or 423 nm. This area is obscured by the very large Soret band in myoglobin and it is not possible to determine whether the peak is present. However, it is possible that absorbances at both positions interfere with the observations of ligation processes at very early times (<3 ps). Because the ground-state spectrum appears as the excited-state spectrum disappears in RNCHm* it is expected that this will occur with ImHm* and Mb* as well. In this case they absorb at similar wavelengths, and the change is therefore not as large as it is in the case of RNCHm*. Since this species does not recombine it will slow the collapse but not the diffusion, causing a small error in quantum yield, but cancelling to some extent the error its presence introduces in rate of decrease of the long wavelength absorbance due to collapse (k_{-1}). This means that the excited-state decay will not interfere with geminate rates significantly if the geminate processes are much slower than excited-state decay.

(16) Dixon, D. W.; Kirmaier, C.; Holten, D. *J. Am. Chem. Soc.* **1985**, *107*, 808–813.

(17) (a) Momenteau, M.; Lavalette, D. *J. Am. Chem. Soc.* **1978**, *100*, 4322–4324. (b) Lavalette, D.; Tetreau, C.; Momenteau, M. *J. Am. Chem. Soc.* **1979**, *101*, 5395–5401.

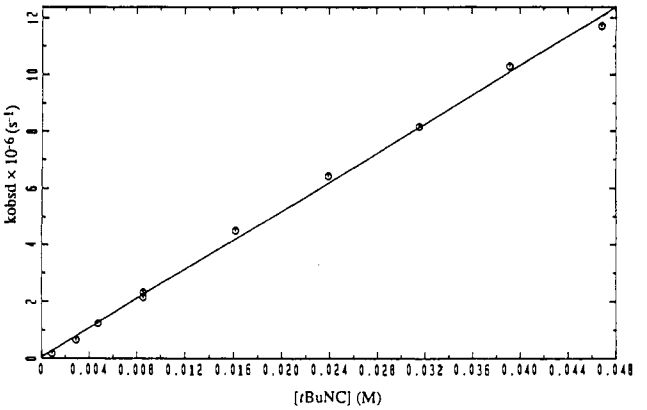

Figure 9. Kinetic plot for the recombination of *t*-BuNC to five-coordinated PHDME(*t*-BuNC) in toluene. The observed first order rate is plotted as a function of [*t*-BuNC]. The bimolecular rate constant from the slope is 2.5×10^8 M^{-1} s^{-1}.

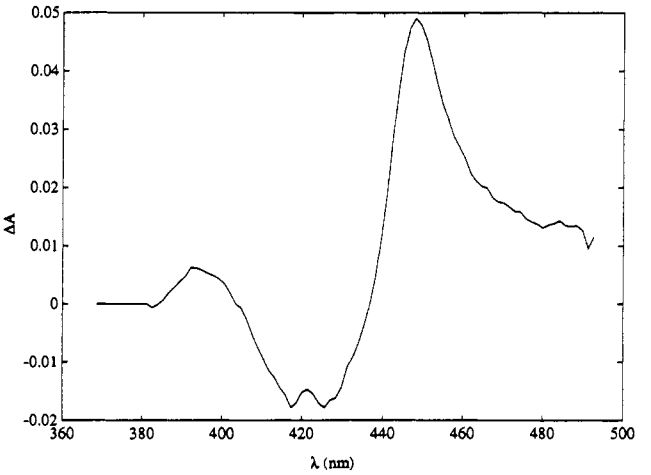

Figure 10. Difference spectrum from subtracting the picosecond transient spectrum at zero time from that at 42 ps after photolysis of protoheme dimethyl ester bis(*t*-BuNC) complex in toluene.

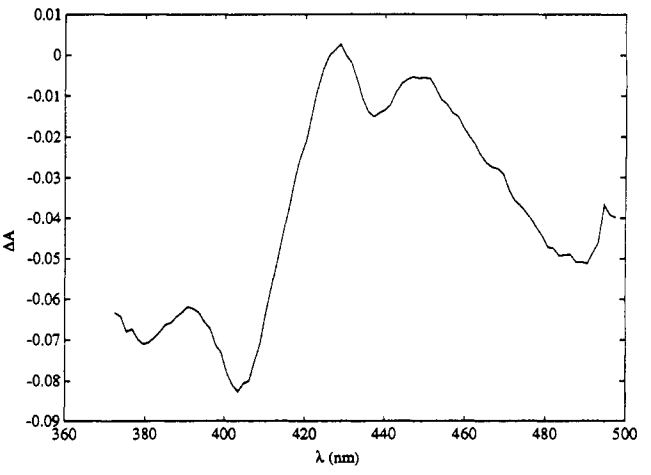

Figure 11. Difference spectrum from subtracting the picosecond transient spectrum at zero time from that at 50 ps after photolysis of protoheme dimethyl ester–1,2-dimethylimidazole–*t*-BuNC complex in toluene.[13a]

In the CO photolysis (eq 10), no cage return is observed because the collapse rate for the heme and CO is too slow.[10a,11c] Thus, the excited-state decay is easily seen. In the bisisocyanide case the cage return is also absent, but the reason is different. At longer times in the pure *tert*-butyl isocyanide solvent, return to bisisocyanide occurs with a rate constant of 3.5×10^9 s^{-1}. At lower *t*-BuNC concentrations this return is absent. Therefore there is no cage return after $(t\text{-BuNC})_2Hm$ photolysis.

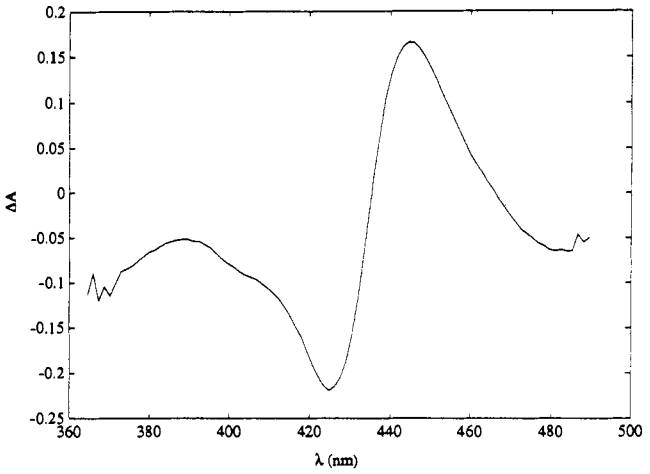

Figure 12. Difference spectrum from subtracting the picosecond transient spectrum at zero time from that at 90 ps after photolysis of myoglobin-CO.[11c]

Table I. Cage Return and Excited-State Decay Rates in the Photolyses of Protoheme Dimethyl Ester Bisisocyanides

R in $Hm(RNC)_2$	% cage[a] return	k^*,[b] s^{-1}	$(k_{-1} + k_2)$,[c] s^{-1}	k_{bimol}, M^{-1} s^{-1}
Me	0	5×10^{10}	none	2.8×10^8
t-Bu(toluene)	0	8×10^{10}	none	2.5×10^8
t-Bu(min·oil)	30	1.4×10^{11}	$\sim 10^{11}$	
α-cholestanyl	95	?	7×10^{10}	
1,1,3,3-tetramethylbutyl	~15	$\sim 10^{11}$	$\sim 10^{11}$	

[a] % recovery of the 432-nm bleaching. [b] Rate constant for disappearance of the 450-nm band or appearance of the 402-nm band. [c] Rate constant for the recovery of the 432-nm absorbance.

The bimolecular rate constant for reaction 12 is 2.5×10^8 M^{-1} s^{-1} (Figure 10). This rate constant is somewhat larger than that

$$(t\text{-BuNC})_2\text{Hm} \underset{2.5 \times 10^8\ M^{-1}\ s^{-1}}{\overset{h\nu}{\rightleftharpoons}} t\text{-BuNCHm} + t\text{-BuNC} \qquad (12)$$

for reaction 13 in which the proximal base is 1-methylimidazole.

$$\text{MeImHm}t\text{-BuNC} \underset{2 \times 10^8\ M^{-1}\ s^{-1}}{\overset{h\nu}{\rightleftharpoons}} \text{MeImHm} + t\text{-BuNC} \qquad (13)$$

In both reactions 12 and 13 the overall bimolecular reaction rate constant is given (referring to eq 2) by $k_{obs} = (k_{-2}\,k_{-1})/(k_2 + k_{-1})$. Since there is more than 50% cage return after photolysis of 1-MeImHm*t*-BuNC or other imidazole–heme–isocyanide complexes[11a] and because both k_{-2} and k_2 should be the same for the species of eq 12 and 13, we can predict at least 50% return of the ground-state contact pair (eq 14).

$$\text{RNC} + \text{RNCHm} \overset{k_2}{\longleftarrow} [\text{RNCHm CNR}] \overset{k_{-1}}{\longrightarrow} \text{RNCHmCNR} \qquad (14)$$

We conclude that the excited state Hm*t*-BuNC* does not combine with *t*-BuNC. The isocyanide apparently diffuses out of the cage faster than the heme relaxes to the ground state ($k_2 > k^*$) (eq 15). These findings suggest that in general an excited

$$[t\text{-BuNCHm}^*\ t\text{-BuNC}] \xrightarrow{k_2} t\text{-BuNCHm}^* + t\text{-BuNC} \qquad (15)$$
$$\qquad\qquad\qquad\qquad\qquad\qquad \xrightarrow{k^*} t\text{-BuNCHm}$$

state HmL* will not add a sixth ligand.

Effect of Ligand Size on Excited-State Decay. In striking contrast to the behavior of *t*-BuNC or MeNC, the photolysis of the heme complex of the much larger isocyanide, $Hm(\alpha ChNC)_2$, shows a direct conversion of the 445-nm band to the six-coordinated product absorbing at 432 nm. This return is around 95%, and there is a ~5% increase in the absorbance at 402 nm, indicating a competition between recombination and excited-state decay. The αChNC complex with chelated protoheme shows about 95% cage return,[13a] and, since the bimolecular rate constant for isocyanide reaction with RNCHm is faster than that with BHm, we expect that ground-state RNCHm should show at least 95% return. This return could result from direct reaction of the excited state. However, in view of the results presented above, a rapid relaxation to the ground-state five-coordinated heme followed by cage collapse seems preferable.

$$\text{Hm}(\alpha\text{ChNC})_2 \xrightarrow{h\nu} [\text{Hm}\alpha\text{ChNC}^*\ \alpha\text{ChNC}] \xrightarrow{\text{fast}} [\text{Hm}\alpha\text{ChNC}\ \alpha\text{ChNC}]$$
$$\qquad\qquad \underset{\sim 95\%}{\overset{k_{-1}}{\longleftarrow}} \qquad\qquad \downarrow k_2\ (\sim 5\%)$$
$$\qquad\qquad\qquad\qquad\qquad\qquad \text{Hm}\alpha\text{ChNC} + \alpha\text{ChNC} \qquad (16)$$

We attribute the rapid relaxation of the excited state to some interaction between the large isocyanide and the heme. In other studies we noticed an increased affinity of this isocyanide for the heme suggesting some interaction in addition to the Fe–CNR bond.[13a,18] Since similar results (not shown) were obtained with β-isomer it might be that the proximal RNC is the determining factor.

The bis(*tert*-octyl isocyanide) complex, intermediate in size, is also intermediate in behavior. The five-coordinated ground-state complex, absorbing at 402 nm appears along with the six-coordinated complex, both occurring in the cage.

$$\text{Hm}(t\text{-octylNC})_2 \xrightarrow{h\nu} [t\text{-octylNCHm}^*\ \ t\text{-octylNC}]$$
$$\qquad\qquad \swarrow k_1 \qquad \searrow \qquad (17)$$
$$\qquad [t\text{-octylNCHm}\quad t\text{-octylNC}]$$

As in the case of the αChNC, the return is attributed to cage recombination after the decay to the ground-state HmCNR. This is in accordance with the smaller values of k_2 determined for larger isocyanides.[18] These data are summarized in Table I.

The effect of ligand size on amount of cage return is apparent. Effects on kinetic constants are not easily seen because the changes are small, and the rate measurements are not sufficiently accurate. The fact that a large isocyanide and the viscous solvent, mineral oil, both cause the slow excited-state decay to be converted to geminate recombination strongly suggests some kind of vibronic coupling between large molecules in contact with the heme and the heme itself leading to rapid quenching of the excited state.

We cannot exclude the possibility that the species with the long wavelength absorbance is an excited-state six-coordinated heme which dissociates with a rate constant of 8×10^{10} s^{-1}.

$$\text{Hm}(\text{RNC})_2 \underset{k_x}{\overset{h\nu}{\rightleftharpoons}} \text{Hm}^*(\text{RNC})_2 \longrightarrow [\text{HmRNC CNR}] \longrightarrow \text{HmRNC} + \text{RNC}$$
$$\qquad\qquad \underset{k_{-1}}{\longleftarrow} \qquad (18)$$

However, there are several other facts which provide some evidence against this idea. First, picosecond photolyses of BHmCO systems, which show a fleeting long wavelength absorbance, have been demonstrated to dissociate by Raman spectroscopic changes and by observing CO with picosecond infrared spectroscopy.[4] Secondly, in all cases where the Soret absorbance disappears completely, ligand–heme bond breaking occurs,[4a,9,10,16] generally in less than 1 ps.[10a] Finally, since the *t*-BuNCHm reacts with *t*-BuNC faster than does ImHm and the latter gives >50% cage return after photolysis of *t*-BuNC, we must expect >50% cage return for every $(t\text{-BuNC})_2\text{Hm}^*$ which dissociates to produce a ground-state geminate pair. For these reasons we prefer to interpret our results in terms of a five-coordinated excited state.

(18) Traylor, T. G.; Magde, D.; Luo, J. K.; Walda, K. N. *J. Am. Chem. Soc.*, in press.

If the $Hm(RNC)_2$ and 1-MeImHmCNR and MbCNR all give excited-state five-coordinated species which have rather similar spectra, then we conclude that these excited states involve porphyrin $\pi \rightarrow \pi^*$ transitions which have little contribution from the metal. In this way any excited-state five-coordinated heme would have this same long wavelength absorption.

The rates of decay of the excited state (k^*) are more dependent upon structure. The chelated protoheme obtained upon photolysis of the CO or isocyanide complexes relaxes with a half-life of about 2 ps compared to 8.5 ps for *t*-BuNCHm*. The αChNCHm* appears to relax even faster than does excited-state chelated protoheme*. Excited-state myoglobin (Mb*), obtained from photolyses of MbCO or MbCNR, also relaxes to ground-state Mb, a rate that is similar to that of chelated protoheme*.

These variations of excited-state lifetime with the nature of the fifth ligand suggest caution in interpreting photolyses of LHmCO complexes etc., in which L varies, for example, in cytochrome P450–CO. However, in almost all cases the bleached Soret band in LHm* does not return appreciably during the decay to the ground state. This makes the Soret change a somewhat better indication of geminate return than is the five-coordinated absorption if the latter absorbs in the region of 440–450 nm.

It is not clear why the excited-state heme–isocyanide complex relaxes more slowly than does the excited-state heme–imidazole complex. It has been suggested that the heme–CO[19] and heme–CS[20] complexes, isoelectronic with RNC–heme, are low spin and perhaps planar, whereas the heme-base species is high spin and domed.[20] It therefore seems logical that the excited electronic states are also different. Thus RNC–Hm* might be a triplet state which returns slowly to a singlet ground state. But the electronic basis for these long lived excited states is not clear, and some theoretical work on these complexes is in order.

Finally, these studies confirm the generally accepted proposals that picosecond photolysis of the complex BHmL breaks an L–Hm bond, that return occurs in the cage in competition with diffusion, and that *we can confidently separate excited-state relaxation from geminate return.* This finding should provide a means of studying these excited states.

All kinetics reported here are accurately exponential whether the reaction is excited-state decay, geminate recombination/diffusion, or pseudo-first-order reactions. We see no evidence for the nonexponential decay in these solvents, a matter considered in detail elsewhere.[18]

Acknowledgment. We are grateful to the National Institutes of Health (Grant HL 13581 [Traylor]) and to the National Science Foundation (Grant CHE-9114613 [Magde]) for support.

(19) Wayland, B. B.; Mehne, L. F.; Swartz, J. *J. Am. Chem. Soc.* **1978**, *100*, 2379–2383. Wayland reported the spin state of the five-coordinated Fe(TPP)CO was a singlet. We have made the analogous five-coordinated PHDME-CO and determined that the Soret maximum occurs at 400 nm. Because of the similarities in crystal-field strength of CO and isocyanide and the Soret positions, we have postulated that the five-coordinated PHDME-CNR ground state is a singlet. OEPFe-CS is a singlet.[14]

(20) Scheidt, W. R.; Reed, C. A. *Chem. Rev.* **1981**, *81*, 543–555.

Communications to the Editor

The Use of Self-Assembled Monolayers and a Selective Etch To Generate Patterned Gold Features[1]

Amit Kumar, Hans A. Biebuyck, Nicholas L. Abbott, and George M. Whitesides*

Department of Chemistry, Harvard University
Cambridge, Massachusetts 02138
Received April 13, 1992

The combination of aqueous, alkaline cyanide ion (1 M KOH, 0.1 M KCN) and dioxygen rapidly etches Au(0) (eq 1).[2-4] Self-assembled monolayers (SAMs) of long-chain alkanethiolates

$$4Au + 8CN^- + O_2 + 2H_2O \rightarrow 4[Au(CN)_2]^- + 4OH^- \quad (1)$$

on the surface of the gold block this etching. Using a number of techniques—micromachining, microwriting, electron-beam lithography, ion-beam lithography—it is possible to form patterns of SAMs on the Au surface. By combining these techniques for forming patterns with selective etching using the CN^-/O_2 solution, high-resolution patterns of gold on silicon can be fabricated with dimensions as small as 1 μm.[5]

One procedure used a pen to write patterns of hexadecanethiolate[6] as monolayers on Au substrates. The pen, filled with hexadecanethiol, was clamped to a X–Y micrometer, and the gold sample was moved across the tip of the pen at 100–1000 μm/s.[7] This system allowed the formation of 1–100 μm features. Only the drop of thiol (i.e., not the tip of the pen) was in contact with the gold surface. Etching resulted in complete removal of the underivatized Au and underlying Ti.[8,9]

Figure 1 shows a representative line. The regions of the Au surface protected by the SAM exhibited little pitting (fewer than 5 pits, approximately 1 μm in diameter, per mm^2): the density of pitting did not increase for exposures of an additional 12 h. The monolayer was not removed: profilometry confirmed that the thickness of the protected Au was the same before and after immersion in the etching solution. The hydrophobicity of the protected surface (measured by the contact angle of water) did not change. Two-point conductivity measurements indicated that lines having widths of 10 μm were electrically conducting: there were no breaks in the gold over distances of 1–2 cm. Adjacent, unconnected lines spaced apart by 1–2 mm were electrically

(1) This research was supported in part by the Office of Naval Research and the Defense Advanced Research Projects Agency.

(2) Brittan, A. M. *Am. Sci.* **1974**, *62*, 402.

(3) Puddephatt, R. J. *The Chemistry of Gold*; Elsevier: Amsterdam, 1978.

(4) Cotton, F. A.; Wilkinson, G. *Advanced Inorganic Chemistry*, 4th ed.; Wiley: New York, 1980; p 966.

(5) Conventional methods of gold pattern fabrication: Muller, R. S.; Kamins, T. I. *Device Electronics for Integrated Circuits*, 2nd ed.; Wiley: New York, 1986.

(6) Hexadecanethiol is the longest chain alkanethiol that is liquid at room temperature and was the best for writing lines. The thiolate monolayer should be autophobic. Autophobic alkanethiol "ink" allowed smooth formation of continuous lines without leaving excess thiol on a line and without loss of definition through reactive spreading. We used a Staedtler pen.

(7) The gold film (2000 Å in thickness) was prepared by electron beam evaporation onto a titanium-primed (100 Å Ti) silicon wafer.

(8) The etch solution consisted of 1 M KOH and 0.1 M KCN in distilled water. The solution container was open to the ambient air and stirred vigorously. Alternatively, the solution was saturated with dioxygen using a coarse frit. For samples of Au used within 1 day of preparation, we observed no significant difference in resolution or rate of etching using either etch solutions that were saturated with oxygen or those that were not. For such fresh samples, etching was complete in 10–15 min for thin (500 Å) Au films and in 30–45 min for thicker (2000 Å) films. When samples were used several days after preparation, the rate of etching, when dioxygen was not bubbled through the solution, was slower by factors of 5 to 10 than when it was. We assume the slowed etching reflected adsorption of adventitious organic impurities on the surface. After removal of the sample from the etch solution, it was rinsed with distilled water and ethanol and dried in a stream of nitrogen. It was not necessary to control parameters such as temperature and stirring rate rigorously.

(9) The Au and Ti in the regions not protected by the SAM dissolved completely, as determined by energy dispersive X-ray spectroscopy (EDX).

0002-7863/92/1514-9188$03.00/0